Crystallographic and Thiol-Reactivity Studies on the Complex of Pig Muscle Phosphoglycerate Kinase with ATP Analogues: Correlation between Nucleotide Binding Mode and Helix Flexibility†

Zoltán Kovári,‡,§ Beáta Flachner,|| Gábor Náray-Szabó,‡ and Mária Vas*,||

Eötvös Loránd University, Department of Theoretical Chemistry, H-1518, Budapest 112, P.O. Box 32, Hungary, Gedeon Richter Ltd., Department of Computer Assisted Drug Discovery, H-1475, Budapest, 10. P.O. Box . 27, Hungary, and Institute of Enzymology, Biological Research Center, Hungarian Academy of Sciences, H-1518 Budapest, P.O. Box 7, Hungary

Received March 15, 2002; Revised Manuscript Received May 20, 2002

ABSTRACT: Crystal structure of the ternary complex of pig muscle phosphoglycerate kinase (PGK) with the substrate 3-phosphoglycerate (3-PG) and the Mg^{2+} complex of β,γ-methylene-adenosine-5′-triphosphate (AMP−PCP), a nonreactive analogue of the nucleotide substrate, MgATP, has been determined by X-ray diffraction at 2.5 Å resolution. The overall structure of the protein exhibits an open conformation, similar to that of the previously determined ternary complex of the pig muscle enzyme with β,γ-imido-adenosine-5′-triphosphate (AMP−PNP) in place of AMP−PCP (May, Vas, Harlos, and Blake (1996) *Proteins 24,* 292−303). The orientation and details of interactions of the nucleotide phosphates, however, show marked differences. The β-phosphate is linked to the conserved Asp 218, i.e., to the N-terminus of helix 8, through the Mg^{2+} ion; the previously observed interactions of the metal complex of AMP−PNP or ADP with the conserved Asn 336 and the N-terminus of helix 13 are completely absent. These structural differences are maintained themselves in solution studies. Inhibition and binding experiments show a slightly weaker interaction of PGK with MgAMP−PCP than with MgAMP−PNP: at pH 7.5, the K_d values are 1.07 ± 0.18 and 0.41 ± 0.08 mM, respectively. The difference is further enhanced by 3-PG: the K_d values are 2.80 ± 0.66 and 0.68 ± 0.11 mM, respectively. Thus, the previously observed weakening effect of 3-PG on nucleotide binding (Merli, Szilágyi, Flachner, Rossi, and Vas (2002) *Biochemisty 41,* 111−119) is more pronounced with MgAMP−PCP. The discordance between substrate analogues also shows up in thiol reactivity studies. In their binary complexes, both ATP analogues protect the fast-reacting thiols of PGK in helix 13 against modification to similar extent. In their ternary complexes, however, which also contain bound 3-PG, the protective effect of MgAMP−PCP, but not of MgAMP−PNP, is largely abolished. This indicates a much smaller effect of MgAMP−PCP on the conformation of helix 13, which is in good correlation with its altered mode of phosphate binding and the ensuing increase in the flexibility of helix 13, as shown by elevated crystallographic *B*-factors. The possible existence of alternative site(s) for binding of the nucleotide phosphates may have functional relevance.

Phosphoglycerate kinase (PGK)[1] is a typical two-domain monomeric enzyme with a deep cleft between the domains of about equal size (*1* and references therein). Crystallographic studies have shown that 3-phosphoglycerate (3-PG) binds to the N-terminal, while the nucleotide substrates, MgATP or MgADP, bind to the C-terminal domain of the enzyme (*2*−*6*). There are several lines of evidence from solution X-ray scattering (*7*−*9*) and X-ray crystallographic studies (*4*, *10*, *11*) for the relative movement of the two domains toward each other during the catalytic cycle.

This large-scale conformational change can bring the two substrates into proximity for a direct phosphotransfer between them. Domain flexibility, thus, seems to be also essential for PGK in accordance with other enzymes, such as members of the kinase family (*12*). Up to now, structural evidence for domain closure has only been provided by two crystallographic studies of PGK ternary complexes, the abortive complex of *Trypanosoma brucei* PGK with 3-PG and MgADP[2] (*10*) and the complex of *Thermotoga maritima* PGK with 3-PG and the Mg^{2+}-complex of β,γ-imido-adenosine-5′-triphosphate (MgAMP−PNP), a nonreactive analogue of MgATP (*11*). In contrast, structural data on binary complexes with a single substrate, i.e., *B. stearother-*

† The financial support provided by the Grant OTKA (T 029208 and T034944) of the Hungarian National Research Fund and the grant by the Higher Education Research and Development Fund (FKFP 0169/2000) are gratefully acknowledged.

* Corresponding author. Tel.: 36 1 466 5633/161. Fax: 36 1 466 5465, E-mail: vas@hanga.enzim.hu.

‡ Eötvös Loránd University.

§ Gedeon Richter Ltd.

|| Hungarian Academy of Sciences.

[1] Abbreviations: PGK, 3-phospho-D-glycerate kinase or ATP, 3-phospho-D-glycerate 1-phosphotransferase (EC 2.7.2.3); GAPDH, D-glyceraldehyde-3-phosphate dehydrogenase (EC 1.2.1.12); PEG, poly(ethylene glycol); AMP−PCP, β,γ-methylene-adenosine-5′-triphosphate; 3-PG, 3-phospho-D-glycerate; AMP−PNP, β,γ-imido-adenosine-5′-triphosphate; Nbs_2, Ellmann's reagent, 5,5′-dithio-bis(2-nitrobenzoic acid).

[2] 3-PG and MgADP can be considered as substrate and product or vice versa, depending on the direction of the reversible enzyme reaction.

10.1021/bi020210j CCC: $22.00
Published on Web 06/21/2002

mophilus PGK with MgADP (*6*) or pig muscle PGK with 3-PG (*4*), have shown largely open conformations, similar to that of the substrate-free horse muscle enzyme (*2*). From these data, the synergetic effect of the two substrates in domain closure has been concluded (*10*).

Although important features of the molecular mechanism of PGK domain closure have already been noted (*10*, *11*, *13*, *14*), fine details of this conformational change are still obscure. To shed light on these, a meticulous comparison of the available PGK structures with different relative domain position is needed. Crystal structures of pig muscle PGK, the object of our investigations, however, have only been obtained with the molecule in the open conformation. The structures of the binary complex with 3-PG (*4*) and a pseudoternary complex obtained by the diffusion of a nucleotide analogue, MnAMP−PNP, into the crystal of the 3-PG binary complex (*15*) have been solved at high resolution; the overall conformation of both are similar and open. Later on, co-crystallization in the presence of 3-PG, MgADP, and inorganic phosphate as precipitant has also yielded crystals of molecules with an open conformation (*14*). This conformational state has been thought to correlate with the mobility of the β-phosphate of MgADP, which does not occupy a well-defined position in the 1.8 Å resolution structure. On the basis of this and other structural considerations, an important role for the phosphate groups in transmitting the nucleotide effect to the most important hinge-point at the β-strand L (situated between helices 13 and 14) that connects the two domains has been deduced (*14*).

In an independent attempt to unveil the closed conformation of pig muscle enzyme, crystals have been grown recently in the presence of 3-PG and the Mg^{2+} complex of another ATP analogue β,γ-methylene-adenosine-5′-triphosphate, MgAMP−PCP, at low ionic strength using PEG as the precipitant (*16*). Commercially available nonreactive ATP analogues, such as AMP−PCP (*17*) and AMP−PNP (*18*), have been used in various studies on different proteins, e.g., refs *19*−*28*, to mimic the physiological ligand, ATP. Of these, only a few provide structural information on the binding of the analogues (*20*, *21*, *27*, *28*), and only one (*28*) can be considered a real comparative study.

In the present work, we have solved the X-ray structure of the new crystalline ternary complex of pig muscle PGK with 3-PG and MgAMP−PCP with the aim of (i) checking the overall conformation of the enzyme molecule and (ii) determining the details of the binding mode of AMP−PCP to compare with AMP−PNP, also including other known protein structures with either of these analogues. Independent enzymological studies have also been carried out in solution to find correlation with the crystallographic data. Namely, (i) the interaction of AMP−PCP and AMP−PNP have been compared in kinetic and binding studies, and (ii) the effect of analogues on the conformation of the hinge-region has been tested by monitoring the reactivity of Cys 378 and Cys379 (*29*), which are located within helix 13 (*14*). These thiols have been found previously to be sensitive to the conformational state of their surroundings (*30*).

MATERIALS AND METHODS

Enzymes and Chemicals. PGK (EC 2.7.2.3) was isolated from pig muscle as described by Harlos et al. (*4*) and stored as a microcrystalline suspension in the presence of ammonium sulfate and 2 mM dithiothreitol. Its activity, determined by D-3-phosphoglycerate and MgATP, varied between 500 and 700 kat/mol. Glyceraldehyde-3-phosphate dehydrogenase (GAPDH, EC 1.2.1.12) was prepared from pig muscle (*31*).

Lactate dehydrogenase, pyruvate kinase, the Na salts of 3-PG, NADH, ATP, ADP, AMP, NADH, and phosphoenolpyruvate were Boehringer products. The Na salt of β,γ-methylene-adenosine 5′-triphosphate (AMP−PCP), and Li salts of β,γ-imido-adenosine 5′-triphospate (AMP−PNP) were purchased from Sigma. The complexes of MgATP, MgADP, MgAMP, MgAMP−PNP, and MgAMP−PCP were formed by adding $MgCl_2$ (Sigma) in high molar excess (25 mM), which assured a practically complete saturation on the basis of their dissociation constants (*18*, *32*−*34*). PEG_{8000} were from Sigma and from Hampton Research, respectively. All other chemicals were reagent-grade commercial preparation. The Ellmann's reagent (Nbs2) and iodoacetamide were obtained from Serva. The latter was re-crystallized from carbon tetrachloride before usage.

Preparation of Enzyme Solutions. Crystals of PGK were dissolved in 20 mM Tris/HCl buffer (pH 7.5) containing 1 mM EDTA, and the mixture was dialyzed against either the same buffer (for enzyme kinetic measurements) or in 50 mM Tris/HCl buffer (pH 7.5) to remove $(NH_4)_2SO_4$. GAPDH solution was desalted in the same way under the lower ionic strength conditions. The dialysis buffer also contained 1 mM dithiothreitol, except for thiol-reactivity studies. For determining protein concentration, A_{280} values of a 1 mg/mL solution of PGK and GAPDH were taken to be 0.69 (*35*) and 1.0 (*36*), respectively, for a 1 cm path length. The molecular mass of PGK was taken to be 44.5 kDa (*37*).

Crystallization. Single crystals of the ternary complex with MgAMP−PCP and 3-PG were grown at 15 °C within a few weeks in hanging drops as described by Merli et al. (*16*). The reservoir solution contained 10mM AMP−PCP, 12 mM $MgCl_2$, and 10mM 3PG in the presence of 27−28% (w/w) PEG8000 at pH 7.0. The characteristics of the crystals obtained and the data collection statistics are summarized in Table 1.

Data Collection and Refinement. X-ray data were collected from a single crystal of size $1 \times 0.5 \times 0.3$ mm^3 in 1° oscillation images using a MAR-research image plate mounted on a Rikagu RU-200 rotating anode X-ray generator. The data were processed first with the MOSFLM package (*38*) to obtain an initial orientation matrix and then with the DENZO package (*39*). The final data set was nearly complete to 2.5 Å, as seen in Table 1. Molecular replacement was carried out using the AMoRe program (*40*) of the Collaborative Computing Project Number 4 (*41*) using the starting model as the structure of the AMP−PNP and 3PG ternary complex of pig muscle PGK (*15*); bound ligands and water molecules were deleted from the coordinate file used. Refinement was carried out in cycles of the X-PLOR package (*42*), together with manual rebuilding of the model at the end of each cycle using O (*43*). A random set of the reflections (5%) was excluded from the refinement and was used to calculate R_{free}. The 2Fo-Fc map calculated at the first stage of refinement clearly showed the position of the bound substrates and the open conformation of the enzyme. This was followed by cycles of positional refinement, simulated

Table 1: Data Collection and Refinement Statistics

Data Collection	
space group	$P2_1$
unit cell	$a = 36.6$ Å, $b = 110.3$ Å, $c = 48.0$ Å, $\beta = 93.9°$
unique reflections	12274
completeness (%)	90.88 (63.18)[a]
mean $I/\sigma(I)$	7.0 (2.2)[a]
$R_{merge}(I)$ (%)[b]	8.1 (25.2)[a]
Refinement	
resolution range (Å)	20.0−2.50
no. of observations	12274
no. of unique reflections	11956
R (%)[c]	17.30
R_{free} (%)[d]	25.24
average B (Å^2)	25.60
protein main chain (1664)[e]	24.11
protein side chain (1368)[e]	27.02
water (88)[e]	26.27
3-PG (11)[e]	27.26
AMP−PCP (32)[e]	40.14
rmsd bond lengths (Å)[f]	0.004
rmsd bond angles (deg)[f]	0.842
rmsd dihedral angles (deg)[f]	27.050
rmsd impropers (deg)[f]	0.500
Ramachandran Plot Quality[f]	
% in core regions	88.8
% in allowed regions	10.9
% in generously allowed regions	0.3

[a] Numbers in parentheses denote values in the highest resolution shell (2.50−2.61 Å), [b] $R_{merge} = \Sigma_{hkl}\Sigma_i|\langle I(hkl)\rangle - I(hkl)_i|/\Sigma_{hkl}\langle I(hkl)\rangle$, where $I(hkl)_i$ is the measured diffraction intensity and $\langle I(hkl)\rangle$ is the mean intensity. [c] R-factor $= \Sigma_{hkl}|F_{obs}(hkl) - F_{calc}(hkl)|/\Sigma_{hkl}|F_{obs}(hkl)|$. [d] R_{free} is the R-factor for a test set comprising 5% of the data selected randomly. [e] Numbers in parentheses denote the number of non-hydrogen atoms. [f] The stereochemistry was assessed with X-PLOR (*42*) and PROCHECK (*59*).

annealing and grouped anisotropic *B*-factor refinement. For each amino acid residue, the side chain and main chain atoms were grouped separately. AMP−PCP was divided into three groups, the adenine ring, the sugar moiety and the phosphates, respectively. 3-PG was divided into two groups, the phosphate and the rest of the molecule. After each cycle of *B*-factor refinement, the model was inspected and adjusted to the electron density maps. After the first cycle of refinement, substrate molecules AMP−PCP and 3-PG were included in the model. After additional refinement cycles water molecules were added to (i) stereochemically acceptable positions suggested by Waterpick (in X-PLOR) and (ii) positions with acceptable electron density. Bulk solvent corrections were applied at a later stage in the refinement. Only side chains with acceptable density were included in the model; side chains with unacceptable density were shortened according to the density map. Main chain atoms are defined well by the electron density map throughout the sequence, but residues 28−32 (surface loop) have poor side chain densities. Other poor side chain densities were only observed for individual residues, but not for an entire region.

The protein coordinates have been deposited in the Protein Data Bank with accession number 1KF0. For molecular graphics, the Insight II (Biosym/MSI, San Diego, CA) and the Sybyl 6.7 (Tripos Inc., St. Louis, MI) softwares were used.

Enzyme Kinetic Studies. The activity of PGK was measured with 3-PG and MgATP as substrates in 20 mM Tris/HCl buffer (pH 7.5 or 8.5) containing 1 mM EDTA and 1 mM dithiothreitol, at 20 °C. In the assay, oxidation of NADH by the reaction product in the presence of GAPDH was followed spectrophotometrically at 340 nm, as described by Tompa et al. (*30*). For testing the inhibition of various MgATP analogues, enzyme activity was determined both in their absence and presence at varying concentrations of MgATP. The kinetic constants were evaluated by using the following equation, which also takes the activation by an excess of substrate into account (*37*):

$$v = v_S \cdot \frac{[S]}{K_{S(cat)} + [S]} + v_S \cdot (a - 1) \cdot \frac{[S]}{K_{S(cat)} + [S]} \cdot \frac{[S]}{K_{S(act)} + [S]} \quad (1)$$

where v is the measured activity, v_S stands for the hypothetical activity at substrate saturation in the absence of activation, [S] is the substrate concentration, $K_{S(cat)}$ and $K_{S(act)}$ are the binding constants of the substrate to the catalytic and activating sites, respectively, and a is the activation factor. The inhibitory constant (K_I) was calculated from $K_{S(cat)}$ and the apparent $K^{app}_{S(cat)}$ determined in the absence and presence of inhibitors, respectively, using eq 2:

$$K_I = \frac{K_{S(cat)}[I]}{K^{app}_{S(cat)} - K_{S(cat)}} \quad (2)$$

where [I] is the inhibitor concentration.

Kinetic Measurements of Thiol-Reactivity toward Nbs_2. The experiments with PGK were carried out in 50 mM Tris/HCl buffer, pH 7.5, containing 1 mM EDTA, at 20 °C in absence and presence of substrates and their analogues. The reaction was started by adding equimolar or excess of Nbs_2 and followed by measuring the change of absorbance at 412 nm, as described earlier (*29*). During the time of reaction of the freely accessible fast-reacting thiols (2 per mole PGK), the reaction of the other inaccessible thiols (5 per mole) is negligible.

The amount of thiols reacted were calculated by using $\epsilon_{412} = 14\,150$ M^{-1} cm^{-1} (*44*, *45*); approximately 1.5−2.0 mol per mole fast-reacting thiols were found.

Dissociation constants were determined by measuring the rate constant of thiol modification at different concentrations of the investigated ligand. The extent of protection against modification is proportional to the amount of enzyme−ligand complex formed, which allows calculation of K_d by fitting the experimental points with the following equation:

$$Y = k_{max} - \frac{(k_{max} - k_{min})[L]}{K_d + [L]} \quad (3)$$

where Y is the fractional saturation, k_{max} and k_{min} are the rate constants of thiol modification in the absence of, or saturation with, the ligand, [L] is the free ligand concentration (here it can be replaced by the total ligand concentration, as the enzyme-bound ligand is negligible under the experimental conditions), and K_d is the dissociation constant.

Kinetic Measurements of Alkylation by Iodoacetamide. PGK was alkylated with iodoacetamide under pseudo-first-order conditions, i.e., with a high molar excess of the

alkylating agents, in 50 mM Tris/HCl buffer, pH 7.5 at 20 °C. Under these conditions, the two reactive cysteinyl residues are selectively modified, which is accompanied by the loss of enzyme activity (*46*). Kinetics of alkylation was followed by determining residual PGK activity in aliquots withdrawn from the reaction mixture at appropriate time points (*30*). The concentration of iodoacetamide was determined by using the molar absorption coefficient of $\epsilon_{275} = 373\ M^{-1}\ cm^{-1}$ (*47*).

RESULTS

*Crystal Structure of the PGK*MgAMP−PCP*3-PG Ternary Complex*

Crystals of space group $P2_1$ of pig muscle PGK were obtained in the presence of the substrate 3-PG and the MgATP analogue, MgAMP−PCP. X-ray diffraction data from these crystals have led to a refined structure of this ternary complex at 2.5 Å resolution with $R = 17.3\%$ and $R_{free} = 25.2\%$. The electron density map clearly defines the position of most of the protein side chains, as well as the substrate positions (cf. Methods).

Overall Protein Conformation as Compared to the Previous Structures. The gross feature of the new ternary complex and the positions of the bound ligands are shown in Figure 1 (red) in superimposition with the previously determined structures of pig muscle PGK. The binary complex with 3-PG (*4*) (Figure 1A, cyan) and the ternary complex with 3-PG*MnAMP−PNP (*15*) (Figure 1B, green) are superposed separately with the present structure according to the core β-strands of the N- and the C-terminal domain, respectively. Figure 1A also includes superimposition with a recently solved completely open structure (2.7 Å resolution) of the substrate-free pig muscle PGK (black traces), crystallized from citrate (Kovári, Náray-Szabó & Vas, unpublished). In addition, the largely closed structure of the ternary complex of *Thermotoga maritima* PGK with bound 3-PG and MgAMP−PNP (blue) (*11*), crystallized under similar conditions, is shown for comparison in Figure 1B.

As seen, the protein molecule in the new ternary structure of pig muscle PGK (red) adopts an essentially open conformation, not very different from either the 3-PG binary (cyan in Figure 1A) or the 3-PG*MnAMP−PNP ternary (green in Figure 1B) complexes of the same enzyme. The two domains and their bound ligands are rather far away from each other, in contrast to the closed conformation represented by *T. maritima* PGK (blue in Figure 1B). Little differences, however, in the exact level of opening can be identified among the pig muscle PGK structures. For example, a very open form is adopted by the molecule without ligands (black), as also noticed earlier in relation to the slightly closed structure of 3-PG binary complex (*4*).

Binding Details of MgAMP−PCP. While 3-PG binding is similar to binding of other PGK complexes of various origin (*4*, *11*, *48*), striking differences can be observed in the nucleotide binding. The adenine ring and the ribose moiety bind as usual (*6*, *11*, *15*, *48*), but the phosphate chain of MgAMP−PCP folds back to the C-domain and does not extend toward the 3-PG binding site, as expected. Although the averaged (grouped) *B*-factor value (cf. Methods) of the whole AMP−PCP molecule is relatively high (Table 1),

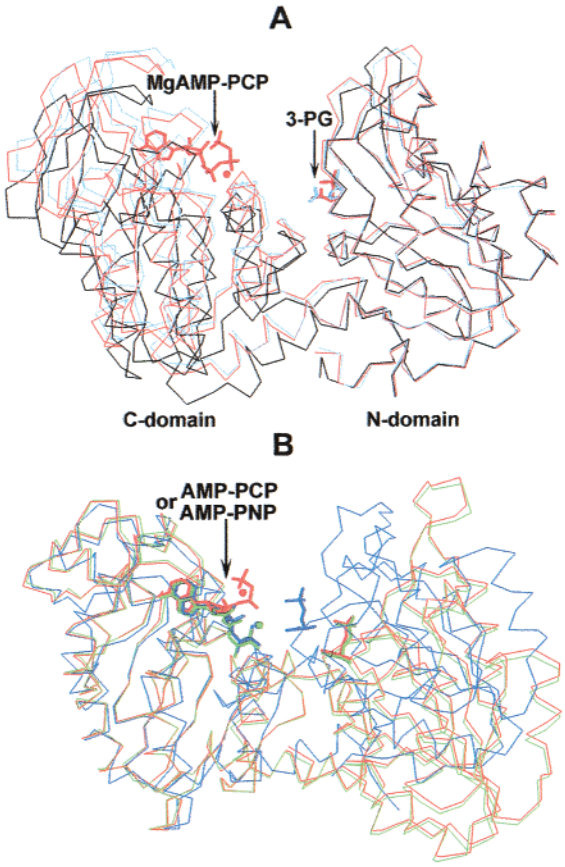

FIGURE 1: Comparison of the complex of pig muscle PGK with MgAMP−PCP*3-PG with other known structures. The Cα traces of PGK structures with the stick model of bound ligands are shown: the present ternary complex with MgAMP−PCP and 3-PG (red), the binary complex with 3-PG (cyan) (*4*), the ternary complex with MnAMP−PNP and 3-PG (green) (*15*), and the substrate-free enzyme (black) from pig muscle (Kovári, Náray-Szabó, and Vas, unpublished data), as well as the ternary complex of *T. maritima* PGK with MgAMP−PNP and 3-PG (blue) (*11*). The present structure was superimposed either with the 3-PG binary complex and the substrate-free enzyme according to the backbone atoms of the core β-strands of the N-domain (A) or, in the same way, with both AMP−PNP-containing ternary complexes according to the C-domain (B).

those of the adenine moiety and the ribose part are only 18.4 and 31.1 Å^2, respectively, which argue in favor of full occupation of the nucleotide-site. Keeping this in mind, the much higher *B*-factor (63.1 Å^2) of its phosphate chain and the attached Mg^{2+} ion indicates an increased mobility of this part of the molecule. On the other hand, the electron density map shows clear orientation of the triphosphate chain. This orientation is surprisingly new and is not seen in any of the nucleotide containing PGK complexes determined so far (*6*, *10*, *11*, *15*, *48*).

The identification of the Mg^{2+} ion requires some caution since its electron density is rather weak and its *B*-factor is rather high (a value of 54 Å^2 was obtained when individual *B*-factor refinement was used). Furthermore, the coordination sphere of the postulated Mg^{2+} is only partially occupied by two ligands: the carboxylate O-atom of the conserved Asp 218 and an O-atom of the nucleotide β-phosphate. Despite these uncertainties, the assumed position of Mg^{2+} ion is approved by its characteristic coordination distances, which are shorter than the usual H-bond (*49*). In addition, the position of the two coordinating ligands corresponds better

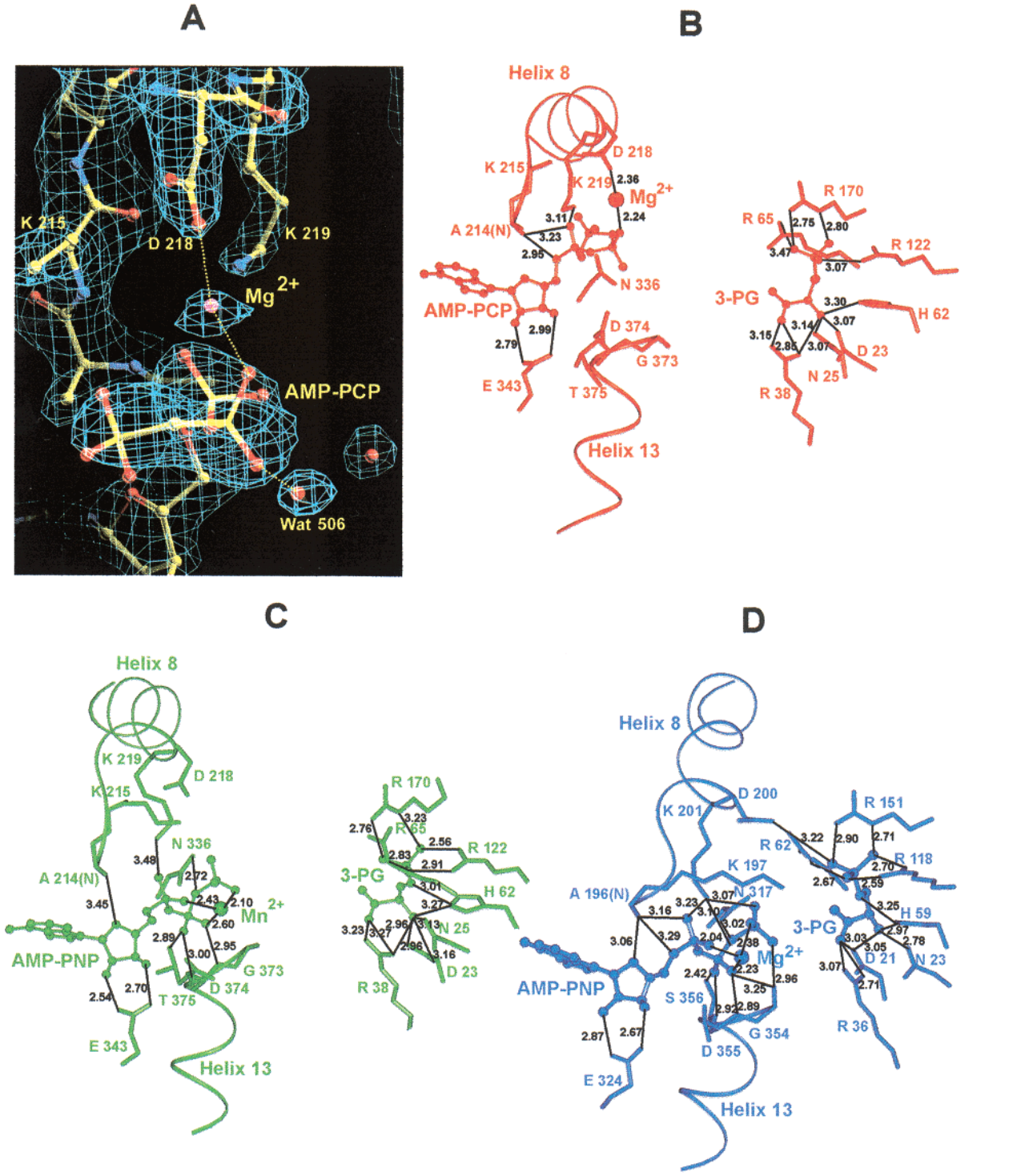

FIGURE 2: Interactions of AMP−PCP in the present structure in comparison with those of AMP−PNP in the previous PGK structures.The 2Fo-Fc electron density map, contoured at 1.1 σ around the phosphates of AMP−PCP bound in the present ternary complex (A), and the ball-and-stick model of both this analogue and 3-PG as well as its surroundings colored in red (B) are shown in comparison with similar illustrations of AMP−PNP as bound in the known ternary complexes of pig muscle (green) (*15*) (C) and of *T. maritima* (blue) PGKs (*11*) (D).

to an octahedral coordination sphere (characteristic of Mg^{2+}), than to a tetrahedral (characteristic to a H_2O molecule).

Accordingly, the indirect ligation of the nucleotide β-phosphate (through Mg^{2+}) to Asp 218 represents a new type of nucleotide−metal−protein interaction of PGK. Interestingly, the completely conserved Lys 215, which is part of the nucleotide-binding region, does not interact with this analogue, as no significant density could be observed around the terminal part of the side chain. The position of Lys 215, otherwise, would allow an interaction with the closely located nucleotide γ-phosphate, which does not form any contact with the protein in this structure. The other conserved lysine (Lys 219) that affects nucleotide binding has a well-defined electron density map around its side-chain. Its terminal N-atom stabilizes the phosphate chain of the nucleotide analogue by connecting an α-phosphate oxygen with a distance of 3.11 Å (Figure 2B), in a way similar to all other PGK complexes (cf. also Figure 2C,D). The phosphorus atom

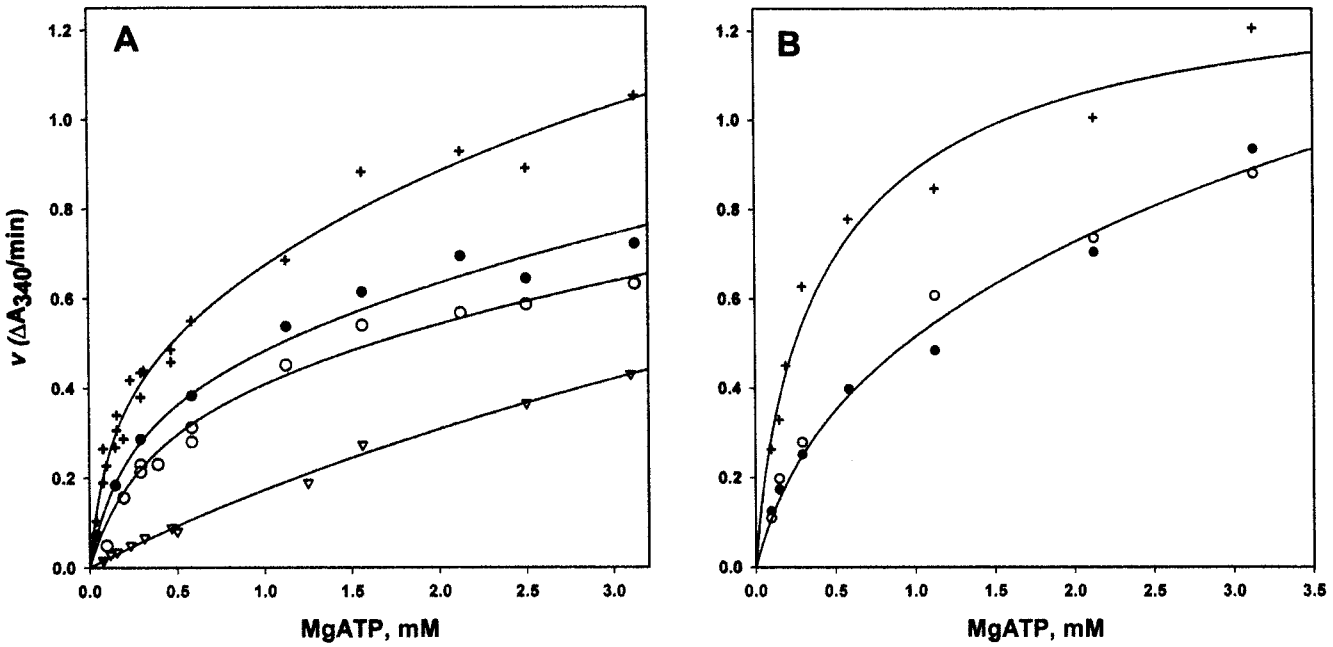

FIGURE 3: Inhibition of PGK activity by the nucleotide analogues at different pH's. The activity (v) of 7 nM enzyme was measured in the presence of 5 mM 3-PG, 25 mM $MgCl_2$, and various concentrations of ATP at pH 7.5 (A) and pH 8.5 (B). The measurements were carried out in the absence of inhibitor (+) and in the presence of 1.5 mM MgAMP−PCP (●), 1.5 mM MgAMP−PNP (○), and 0.94 mM MgADP (▽). The experimental points were fitted to eq 1 given in the Methods section. The inhibitors did not seriously influence the values of v_S, a, and $K_{S(act)}$, and for these terms, 0.5 ± 0.15 ΔA_{340}/min and 4.0 ± 1.3 and 6.3 ± 2.8 mM, respectively, were obtained, independent of the pH. The inhibitors influenced the value of $K_{S(cat)}$ for which 0.106 ± 0.054 mM was obtained in the absence of inhibitors, at both pH's. From this value and the apparent $K^{app}_{S(cat)}$ determined in the presence if inhibitors the inhibitory constants (K_I) were calculated by using eq 2 of the Methods; the values are given in Table 2.

of the γ-phosphate is 15.1 Å away from the 3-PG carboxyl O-atom, while the corresponding distance is 10.1 Å in the MnAMP−PNP ternary complex of the pig muscle enzyme (not marked in the figures): neither of these distances would allow phosphate transfer to occur, which requires about 5 Å (*50*).

While the phosphate chain strongly interacts with helix 8, practically no interactions are observed with helix 13 (Figure 2B). In contrast, in the other known ternary complexes containing MnAMP−PNP bound to the open structure of pig muscle PGK (Figure 2C) or MgAMP−PNP bound to the closed structure of *T. maritima* PGK (Figure 2D) or even in the binary complex with MgADP of *B. stearothermophilus* PGK (*6*) (not shown), well-formed interactions exist with helix 13. It should be noted that substitution Mn^{2+} for Mg^{2+} into has no influence on nucleotide binding, as the bivalent metal ion required by PGK catalysis can be replaced by other metals, most notably by manganese, under physiological conditions (*51*).

Enzymological Studies with the Solubilized PGK Using AMP−PCP and AMP−PNP

Inhibitory Effect of the Analogues. Figure 3 shows kinetic data obtained with the two nucleotide analogues. The nonhyperbolic dependence of PGK activity on the concentration of the nucleotide substrate, MgATP, can be described by the same type of kinetic equation published earlier for saturation with the other substrate, 3-PG (*37*), i.e., by assuming the existence of a stronger catalytic and a weaker regulatory site for the substrate. The analogues MgAMP−PCP and MgAMP−PNP inhibit the reaction by mainly increasing $K_{S(cat)}$, i.e., weakening MgATP binding to the catalytic site, and only slightly influencing $K_{S(act)}$, the binding constant of MgATP to the secondary activating site. At pH 7.5, MgAMP−PNP inhibits somewhat more strongly than MgAMP−PCP (Figure 3A), while at pH 8.5, their inhibitory effects became similar (Figure 3B). By assuming a competitive replacement of MgATP by its analogues, their inhibitory constants (K_I) have been calculated (Table 2). While the values for the two analogues are different at pH 7.5, they are uniformly 0.59 ± 0.23 mM at pH 8.5 for both. The pH effect correlates with the higher pK_a of the last dissociating proton from the phosphate-group of AMP−PCP as compared to that of AMP−PNP (8.4 vs 7.7, as given by ref *18*). As a comparison, the inhibitory effect of the nucleotide product, MgADP, has been also investigated at pH 7.5 and shown in

Table 2: Inhibitory Constants (K_I) of Various Nucleotides on the PGK-Catalyzed Reaction in Comparison with the Dissociation Constants (K_D, mM) of Their Binding to PGK[a]

		K_d (mM)	
nucleotide	K_I (mM)	no 3-PG	10 mM 3-PG
MgAMP−PCP	1.21 ± 0.24	1.07 ± 0.18 1.28 ± 0.42[b]	2.80 ± 0.68
MgAMP−PNP	0.58 ± 0.28	0.41 ± 0.08 0.43 ± 0.21[b]	0.68 ± 0.11
MgADP	0.039 ± 0.012	0.039 ± 0.014 0.060 ± 0.01[c,d]	0.31 ± 0.040 0.38 ± 0.038[d]

[a] The inhibitory constants have been obtained from kinetic measurements shown in Figure 3A using eqs 1 and 2. The dissociation constants have been derived from measuring the extent of protection against thiol modification with Nbs_2, as examplified by the curves in Figure 4. The curves are fitted by eq 3. The experimental conditions are 20 or 50 mM Tris buffer, pH 7.5, 1 mM EDTA, 25 mM $MgCl_2$, 20 °C. [b] Data from equilibrium dialysis binding studies (obtained under similar experimental conditions): Szilágyi & Vas, unpublished. [c] (*53*). [d] (*16*).

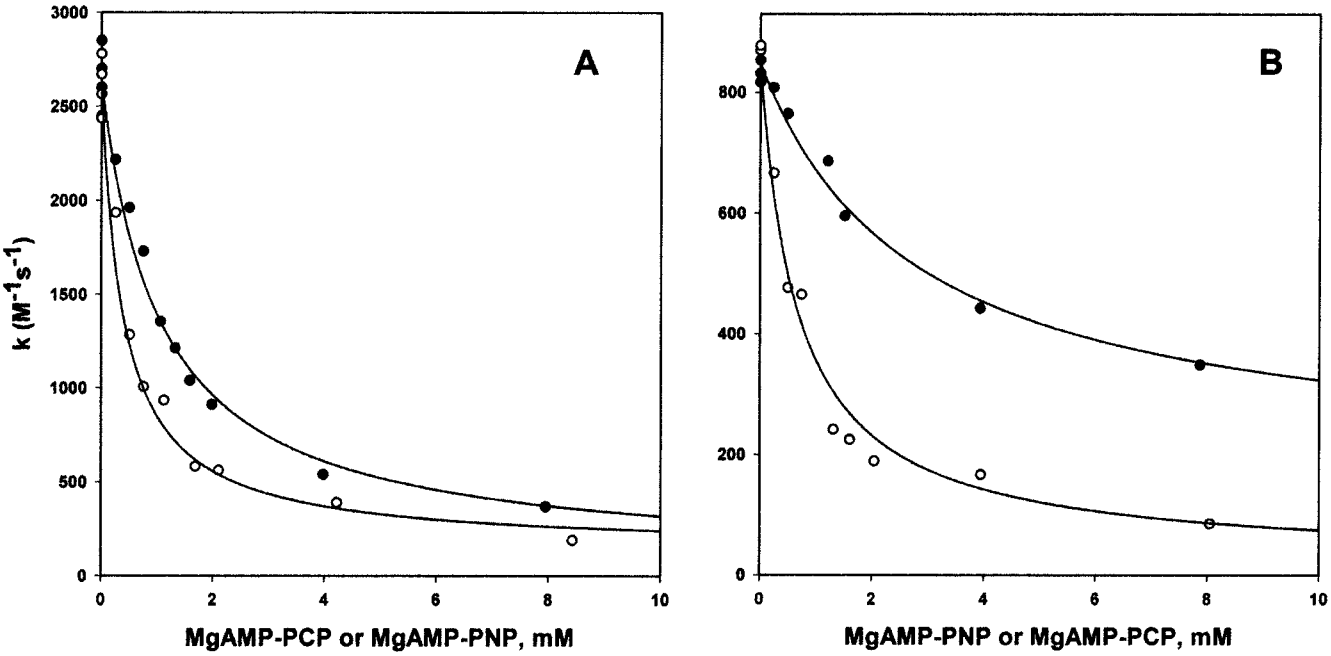

FIGURE 4: Concentration-dependent protection of MgAMP−PCP and MgAMP−PNP against modification of PGK with Nbs_2. The accessible thiol groups of 9 μM PGK were reacted with various constant concentrations of Nbs_2 (in the range of 0.02−0.1 mM) in the presence of different concentrations of each of the nucleotide analogues both in the absence (A) and in the presence (B) of 10 mM 3-PG. 25 mM $MgCl_2$ was present throughout the experiments. The time course of modification was recorded at 412 nm and analyzed using the first-order rate equation. The rate constants are plotted as a function of nucleotide concentration. The filled and open symbols refer to the data with MgAMP−PCP and MgAMP−PNP, respectively. Curve fitting was carried out by using eq 3 of the Materials and Methods section. While keeping the k_{max} values to 2625 (A) and 847 (B) $M^{-1}s^{-1}$, the fitted k_{min} values, characteristic of the maximal protecting effect of MgAMP−PCP and MgAMP−PNP, are 72 ± 96 and 145 ± 108 $M^{-1}s^{-1}$ in the absence of 3-PG (A) and 177 ± 65 and 22 ± 29 $M^{-1}s^{-1}$ in the presence of 3- PG (B), respectively. The fitted K_d values are summarized in Table 2.

Figure 3A. Its much stronger inhibition ($K_I = 0.039 \pm 0.012$ mM) correlates well with its stronger binding to PGK (cf. below).

Binding of the Analogues are Differently Affected by 3-PG. The dissociation constants of MgAMP−PCP and MgAMP−PNP binding to PGK have been determined both in the absence and presence of the substrate, 3-PG, by an indirect method, by a way of measuring thiol-group reactivity of PGK as a function of saturation with the ligand. This method is much more economical than equilibrium dialysis and yields essentially the same K_d values (Table 2). The principle of the determination is that bound ligands largely protect the two adjacent reactive cystein residues (Cys 378 and Cys 379) against modification by the Ellman's reagent, Nbs_2 (*29*). Since the extent of protection is proportional to the complexation of the enzyme, it can be used to follow saturation with the ligand (cf. Methods).

Figure 4 shows the results of these experiments, and the calculated K_d values are summarized in Table 2. While in the absence of 3-PG the binding of MgAMP−PCP is only slightly weaker than that of MgAMP−PNP, possibly due to the lower extent of ionization of its phosphates at pH 7.5 (Figure 4A), in the presence of 3-PG, the differences between the two binding curves become much more pronounced. (Figure 4B). Namely, 3-PG significantly weakens the binding of MgAMP−PCP but has hardly any effect on MgAMP−PNP. Incidentally, 3-PG largely weakens the strong binding of MgADP (Table 2 and refs *16*, *52*, and *53*), which confirms these results.

Different Protection of the Analogues against Modification of the Fast-Reacting Enzyme Thiols. When the protective effect of both analogues against thiol modification is extrapolated to infinite analogue concentrations, closely similar protection was obtained in the binary complexes (Figure 4A). In the presence of saturating concentrations of 3-PG, however, a markedly smaller protection by MgAMP−PCP, than by MgAMP−PNP, was observed (Figure 4B, cf. also Legends to Figure 4). Thus, not only the binding constant, but also the binding mode, of the two analogues become different in the ternary complexes, in agreement with the structural observations.

In general, it has to be emphasized that any bound ligand may affect thiol reactivity by either direct steric hindrance or an indirect effect on local conformation around the reactive residues. Since the Ellmann's reagent is a relatively large molecule, a direct steric hindrance may contribute to the large protection observed. Therefore, we also characterized the protective effect a much smaller reagent, iodoacetamide, already used for similar studies with PGK (*30*). Table 3. summarizes the data obtained with both reagents in the presence of closely saturating concentration of both analogues. As the extent of protection against modification with the two reagents is very similar, it apparently does not depend on the reagent size. Therefore, a direct steric protection by the analogues can be excluded, and their effect is characteristic of the local conformational change around the cysteinyl residues, in line with the previous suggestion (*30*). The absence of a steric protection correlates well with the structural data, which show that the nucleotide P-atoms (in average) are as far as 15 and 12 Å away from the cystein S atoms in the structure with AMP−PCP and AMP−PNP, respectively.

Table 3: Protective Effect of Various Nucleotide Ligands at Saturation against Modification of PGK Thiols by Nbs_2 or Iodoacetamide[a]

	second-order rate constants (k, $M^{-1}s^{-1}$) and their relative values							
	No 3-PG				10 mM 3-PG			
ligand	Nbs_2		iodoacetamide		Nbs_2		iodoacetamide	
none	2625 ± 39	1	0.118 ± 0.017	1	850 ± 19	1	0.047 ± 0.003	1
MgAMP−PCP	319 ± 41	0.121	0.0107 ± 0.0018	0.091	324 ± 23	0.38	0.0147 ± 0.0014	0.312
MgAMP−PNP	240 ± 32	0.093	0.0104 ± 0.0012	0.088	59 ± 14	0.070	0.0044 ± 0.0002	0.093
MgATP	280 ± 30[b]	0.106	0.014[b]	0.120	not measurable[c]		not measurable[c]	
MgADP	22 ± 3[⊥]	0.008	0.0014 ± 0.0006[b]	0.012	18 ± 5	0.021	0.0026 ± 0.0002	0.055

[a] The reaction conditions with Nbs_2 are given in the legends to Figure 4. For alkylation, 1 μM PGK was reacted with various concentrations of iodoacetamide in the range of 10−60 mM in the absence and presence of 10 mM of each of the nucleotides. 25 mM $MgCl_2$ was also present throughout the experiments. Other experimental conditions are 50 mM Tris buffer, pH 7.5, 1 mM EDTA, 20 °C. The second-order rate constants of thiol modification (k, $M^{-1}s^{-1}$) were calculated from the time course of the reactions. The values have been normalized to that obtained in the absence of ligand. [b] Data from ref *30*. [c] Functional ternary complex.

As mentioned above, in the presence of 3-PG, striking differences have been detected between the protective effect of MgAMP−PCP and MgAMP−PNP with both thiol-modifying reagents. These differences only hold the ternary but not the binary complexes. For a comparison, MgADP exerts the largest protection against modification of the fast reacting thiols, as noted earlier (*30*) and it is slightly influenced by 3-PG (Table 3).

DISCUSSION

Relative Position of the Two Domains. The open domain positions in the X-ray structure of pig muscle PGK co-crystallized with the 3-PG and AMP−PCP are similar to previously determined complexes, the crystals of which were grown in the presence of 3-PG (*4*), and the nucleotide AMP−PNP was diffused only later to the pregrown crystal (*15*). The new open structure is fully consistent with predictions made on the basis of indirect binding studies by single-crystal micro-spectrophotometry (*16*). As concluded there, the open conformation of this new ternary complex probably does not represent the average protein conformation in solution. Rather, the source-specific protein−protein interactions operating in the crystal lattice may have selected and stabilized a particular protein conformation, as also discussed for other cases (*54*−*56*).

Yet the open character of the present structure is in contrast to expectations, as co-crystallization with both ligands could have allowed stabilization of the closed form that possibly dominates in solution, as evidenced by solution X-ray scattering (*7*−*9*) and enzyme kinetic (*57*) studies. Thus, besides the source-specific lattice constrains, one might also consider the characteristic binding mode of AMP−PCP, which greatly differs both in location and the binding details of its phosphates from that of AMP−PNP (cf. Figures 1 and 2). This unexpected binding mode of AMP−PCP may lack some details of the enzyme−nucleotide interaction, which are important for stabilizing the domain-closed form. In particular, the absence of any interaction of MgAMP−PCP with the conserved Asn 336 (Figure 2B), due to the noninteracting methylenegroup (cf. below), which contrasts to AMP−PNP binding (Figure 2C). For this reason, the nucleotide-mediated direct contacts of Asn 336 of the core β-strand of the C-terminal domain (Asn 317 in *T. maritima* PGK, cf. Figure 2D) with the conserved Lys 219 (Lys 201 in *T. maritima* PGK) of helix 8 and simultaneously with the peptide O atom of Gly 371 (Gly 352 in *T. maritima* PGK) of helix 13 (not shown), which only exists in the closed forms (*14*), are inherently excluded in the present structure. These interactions, among others, are thought to be important in assisting in the domain closure (*14*). Nevertheless, caution has to be exercised in accepting the conclusion that the absence of a single H-bond (e.g., the one with Asn 336) explains the absence of a closed conformation, in itself.

Orientation of Phosphates of the Bound MgAMP−PCP. The most interesting feature of the new structure is the unprecedented orientation of the bound nucleotide phosphate on the protein surface (Figure 1B). The strikingly different binding mode of MgAMP−PCP (Figure 2B) and MnAMP−PNP (Figure 2C) is apparently not the result of a difference in crystallization protocols (co-crystallization vs diffusion into the pregrown crystal). At least, the binding mode of AMP−PNP depends neither on the way of crystal growing nor on the origin of the enzyme and is independent of the relative domain positions, as exemplified by comparing panels C (pig PGK) and D (*T. maritima* PGK) of Figure 2.

To interpret the binding differences, one should consider that the phosphate chain of AMP−PCP contains a methylene group in place of the oxygen atom between β- and γ-phosphates. This difference alters both the electrostatic and H-bonding potential of the nucleotide analogue; furthermore, the geometry around the corresponding carbon atom differs slightly from that of the oxygen atom. On the other hand, AMP−PNP has a nitrogen-atom-containing imido group in the same position that forms another local environment between the β- and γ-phosphates (*18*).

These inherent differences may be reflected not only in different strength, but also in different mode, of binding of the two analogues. The latter can be facilitated by the flexibility of their phosphate chain. In fact, the phosphate chain can occupy various positions relative to the adenine and ribose rings, as shown by superimposing the analogues bound to various proteins (Figure 5). On the other hand, the almost identical binding mode of AMP−PNP and AMP−PCP to the histidine kinase CheA (*28*) may be consistent with the absence of any interaction of the −NH bridge of AMP−PNP with this kinase.

As for PGK, the present solution inhibitory studies, carried out at different pH's (Figure 3), indicate the importance of the electrostatic interactions in binding of the analogues. The fact that for AMP−PCP a smaller inhibitory effect than for AMP−PNP has been detected at lower pH (7.5) is entirely consistent with the higher pK_a of the last dissociating proton

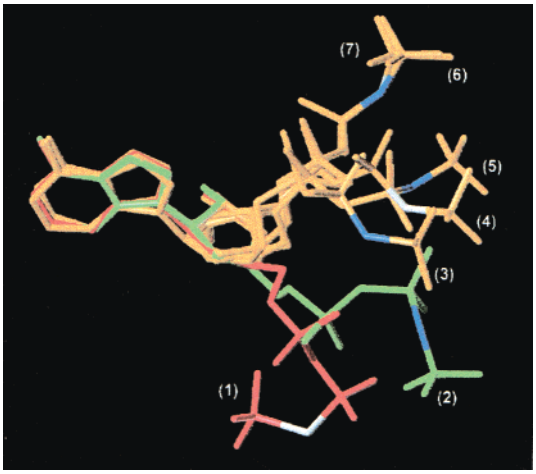

FIGURE 5: Superimposition of the ATP analogues AMP−PCP and AMP−PNP bound to PGK and other proteins Superimposition was done according to the N atoms of the adenine ring and all the heavy atoms of the ribose moiety. The differing heavy atoms between the β- and γ-phosphates of the nucleotide analogues are colored according to the conventional atom codes (C, white, N, blue). All the other heavy atoms of AMP−PCP in the new structure are colored red (1), while those of AMP−PNP in the previously determined MnAMP−PNP*3-PG*PGK ternary complex from pig muscle (*15*) are colored green (2). Similarly, all the other heavy atoms of AMP−PNP bound to *E. coli* adenylate kinase (*21*) (3), of AMP−PCP bound to MinD ATPase (*27*) (4), of AMP−PNP bound to the catalytic subunit of cAMP-dependent protein kinase (*20*) (5), and of AMP−PNP and AMP−PCP bound to histidine kinase CheA (*28*) (6 and 7), respectively) are uniformly colored orange.

of the phosphates of the former (*18*). Further, since the difference in the inhibition disappears at higher pH (8.5), the lack of a H-bond of the methylene-group of AMP−PCP with the protein has no serious influence on the binding constant of this analogue.

The less favorable interaction of AMP−PCP with PGK at pH 7.5 or lower may stem from a less favorable electrostatic interaction of its phosphates with the positively charged N-terminus of helix 13, similar to other helix dipoles (*58*). On the other hand, well-established interactions between the phosphates of AMP−PNP with the N-terminus of helix 13 have been previously observed (*15*, cf. Figure 2C). This explains the weaker binding of MgAMP−PCP relative to MgAMP−PNP, as we actually observed (Table 2).

These considerations, however, may not offer an explanation for the different orientation of the nucleotide phosphates. The experiments in the presence of 3-PG (cf. discussion below) have shed more light on this problem.

3-PG Caused Differences in the Binding Modes of AMP−PCP and AMP−PNP. Nucleotide binding and thiol-reactivity studies have been carried out in solution at lower pH (7.5), where MgAMP−PCP binds more weakly than MgAMP−PNP (Table 2). The difference in their binding is increased by 3-PG, i.e., in the ternary complexes, similar to the one in the crystal (Figure 4 and Table 2). These results are not only consistent with the previously observed antagonistic effect of 3-PG on nucleotide binding (*16*, *52*) but may also be compatible with the different location of the nucleotide phosphate chain observed for the in the crystalline ternary complexes (Figure 1B). Namely, it is conceivable that 3-PG abolishes the weaker interactions of the phosphates of MgAMP−PCP with the protein more easily, and thus they move to the novel site. We have no structural data on MgAMP−PCP binding in the absence of 3-PG, but the present structure together with the solution binding data may support this proposal.

Further evidence for the 3-PG-caused differences between the interaction of the two ATP analogues came from thiol-modification studies. A less pronounced protection of the two reactive thiol groups in helix 13 by the bound MgAMP−PCP relative to MgAMP−PNP has only been observed in the presence of 3-PG (cf. Table 3). This finding correlates well with the crystallographic data of the respective ternary complexes. Since direct steric protection could be excluded by applying reagents of different size, the data relate to the local conformational state. In the new structure, where all the possible interactions of the nucleotide with the N-terminus of helix 13 are absent (Figure 2B), the whole helix becomes more mobile and flexible, as indicated by the elevated *B*-factor values of this region (Figure 6A). Under these conditions, the thiol groups located on this helix are, indeed, more accessible toward modification, as we actually found.

Correlation between the Nucleotide Binding Mode and Helix Flexibility. A close relationship between thiol reactivity, flexibility of helix 13, and the orientation of the bound nucleotide phosphates apparently holds not only in the present ternary complex, but also in other nucleotide-containing complexes of PGK. In the ternary complex containing bound MnAMP−PNP, the phosphate O-atoms are H-bonded to the N-terminus of helix 13 (Figure 2C), extending and stabilizing the H-bond network of the helix. In addition, electrostatic interactions between the negatively charged phosphates and the positively polarized N-terminus of the helix also seem to operate (*15*). In accordance, the mobility of helix 13 in this structure is relatively restricted, as shown by the lower *B*-factor values in Figure 6B. This is the structural basis of the larger maximal protection of MgAMP−PNP against the thiol modification of the PGK ternary complex, as compared to the effect of MgAMP−PCP (Table 3).

In comparison, the much larger protection of the thiol groups by MgADP ((*30*) and Table 3) may correlate with the strongest observed interaction of this nucleotide with PGK (*53* and cf. Table 2). This is due to the interaction with the carboxylate of Asp 374 of helix 13 through Mg^{2+}, as well as to the additional H-bonds and electrostatic interactions of the β-phosphate with the positive end of the helix dipole at its N-terminus (*6*, *58*). As a consequence, helix 13 becomes very ordered in this case, in line with the very low *B*-factor value of this region (Figure 6C), and its thiol groups become much less accessible. In contrast, *B*-factor values for helix 13 attains the highest values in the substrate-free PGK (not shown), and accordingly, its thiols exhibit the highest accessibility toward modification (Table 3). Thus, in general, there is a good correlation between structural observations and the data obtained with the solubilized enzyme.

Significance of the Results with Respect to the Natural Substrate, MgATP. The question arises whether the novel type of binding mode of MgAMP−PCP has any possible relevance to the binding of the physiological substrate, MgATP. The binding mode of MgATP has not yet been determined, but on the basis of its smaller extent of protection

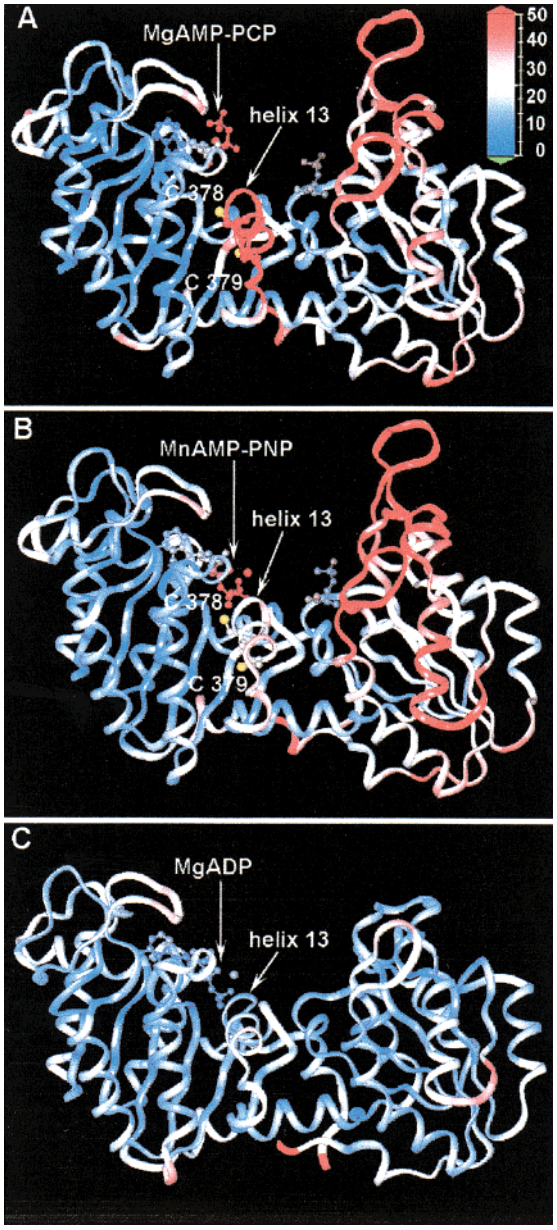

FIGURE 6: Ribbon representation of various PGK*nucleotide complexes colored by the atomic displacement parameter (*B*-factor). The ternary complexes of pig muscle PGK with 3-PG and MgAMP−PCP (present structure, A) and with 3-PG and MnAMP−PNP (*15*, B) and the binary complex of *B. stearothermophilus* PGK with MgADP (*6*, C) are shown. The color code for the crystallographic *B*-factor is shown in the upper right corner of figure (A). The ball-and-stick-model represents the ligands and the nonconserved cysteinyl-residues 378 and 379 in the pig muscle PGK structures. The sulfur atoms are colored yellow, i.e., different from the *B*-factor color code. Note the enhanced difference of *B*-factors between helix 13 and the core C-terminal domain in panel A) as compared to in panel B.

of the thiols as compared to that of MgADP (cf. *30* and Table 3), it may interact weaker with helix 13.

Taken the data together, it is quite possible that in the absence of 3-PG, the phosphates of MgAMP−PCP bind to the N-terminus of helix 13 similarly to but more weakly than MgAMP−PNP. The similarity in the maximal protection on thiol-reactivity by the two analogues in the absence of 3-PG (Table 3), argues for this assumption. Furthermore, in agreement with the proposed molecular mechanism of substrate antagonism (*16*, *52*), 3-PG can abolish the weaker interaction of AMP−PCP more easily, leading to the occupancy of the presently observed novel binding site. The key element of our proposal is that this site represents an alternative for the binding of nucleotide phosphates, which operates only in the presence of 3-PG and possibly also for the substrate MgATP.

The possible significance of an alternative nucleotide site in the enzyme function is beyond the scope of the present work. It is notable that the newly observed site is constituted from the same Asp residue (Asp 218 in pig PGK, equivalent to Asp 200 in *T. maritima* PGK) that interacts with 3-PG and may be important for stabilizing the closed form of *T. maritima* PGK (*11*, cf. Figure 2D). Although no interaction with the other conserved residue (Lys 215) is observed (end of its side-chain is not seen), its transient interaction with the nearby nucleotide phosphates, especially the closest γ-phoshate, transferred during catalysis, cannot be excluded; this would be consistent with a previous postulate (*48*). It is conceivable that during the catalytic cycle a continuous change of atomic positions and interactions within this interdomain region occur. Among them, the fluctuation of nucleotide−phosphates between the two alternative sites may assist domain closure by moving the N-termini of helices 8 an 13 closer to each other, which pertain to the closed form (*14*). The concomitant changes in the flexibility of helix 13 may also contribute to the functioning of the nearby main molecular hinge at the β-strand L. For demonstrating the existence of the proposed alternative site for the physiological substrate, MgATP, further structural studies are in progress.

ACKNOWLEDGMENT

Thanks are also due to A. May and M. Ghosh (Laboratory of Molecular Biophysics, Department of Biochemistry, University of Oxford) for collecting the X-ray diffraction data and for critical remarks, respectively, as well as to V. Harmat (Eötvös Loránd University, Department of Theoretical Chemistry, Budapest, Hungary) for the kind help in the data procession. Critical reading of the manuscript by P. Tompa (Institute of Enzymology, BRC, Budapest, Hungary) is also greatly thanked.

REFERENCES

1. Joao, H. C., and Williams, R. J. P. (1993) *Eur. J. Biochem. 216*, 1−18.
2. Banks, R. D., Blake, C. C. F., Evans, P. R., Haser, R., Rice, D. W., Hardy, G. W., Merrett, M., and Phillips, A. W. (1979) *Nature 279*, 773−777.
3. Watson, H. C., Walker, N. P. C., Shaw, P. J., Bryant, T. N., Wendell, P. L., Fothergill, L., Perkin, R. E., Conroy, S. C., Dobson, M. J., Tuite, M. F., Kingsman, A. J., and Kingsman, S. M. (1982) *EMBO J. 1*, 1635−1640.
4. Harlos, K., Vas, M., and Blake, C. C. F. (1992) *Proteins 12*, 133−144.
5. McPhillips, T. M., Hsu, B. T., Sherman, M. A., Mas, M. T., and Rees, D. C. (1996) *Biochemistry 35*, 4118−4127.
6. Davies, G. J., Gamblin, S. J., Littlechild, J. A., Dauter, Z., Wilson, K. S., and Watson, H. C. (1994) *Acta Crystallogr. D50*, 202−209.
7. Pickover, C. A., McKay, D. B., Engelman, D. M., and Steitz, T. A. (1979) *J. Biol. Chem. 254*, 11323−11329.
8. Ptitsyn, O. B., Pavlov, M. Y., Sinev, M. A., and Timchenko, A. A. (1986) in *Multidomain Proteins* (Patthy, L., and Friedrich, P., Eds.) pp 9−25, Akadémiai Kiadó, Budapest.
9. Sinev, M. A., Razgulyaev, O. I., Vas, M., Timchenko, A. A., and Ptitsyn, O. B. (1989) *Eur. J. Biochem. 180*, 61−66.

10. Bernstein, B. E., Michels, P. A. M., and Hol, W. G. J. (1997) *Nature 385*, 275−278.
11. Auerbach, G., Huber, R., Grättinger, M., Zaiss, K., Schurig, H., Jaenicke, R., and Jacob, U. (1997) *Structure 5*, 1475−1483.
12. Matte, A., Tari, L. W., and Delbaere, L. T. (1998) *Structure 6*, 413−9.
13. Bernstein, B. E., Williams, D. M., Bressi, J. C., Kuhn, P., Gelb, M. H., Blackburn, G. M., and Hol, W. G. J. (1998) *J. Mol. Biol. 279*, 1137−1148.
14. Szilágyi, A. N., Ghosh, M., Garman, E., and Vas, M. (2001) *J. Mol. Biol. 306*, 499−511.
15. May, A., Vas, M., Harlos, K., and Blake, C. C. F. (1996) *Proteins 24*, 292−303.
16. Merli, A., Szilágyi, A. N., Flachner, B., Rossi, G. L., and Vas, M. (2002) *Biochemistry 41*, 111−119.
17. Myers, T. C., Nakamura, K., and Flesher, J. W. (1963) *J. Am. Chem. Soc. 82*, 3292−.
18. Yount, R. G., D. Babcock, Ballantyne, W., and Ojala, D. (1971) *Biochemistry 10*, 2484−2489.
19. Tomaszek, T. A., Jr., and Schuster, S. M. (1986) *J. Biol. Chem. 261*, 2264−9.
20. Bossemeyer, D., Engh, R. A., Kinzel, V., Ponstingl, H., and Huber, R. (1993) *Embo J. 12*, 849−59.
21. Berry, M. B., Meador, B., Bilderback, T., Liang, P., Glaser, M., and Phillips, G. N., Jr. (1994) *Proteins 19*, 183−98.
22. Orokos, D. D., and Travis, J. L. (1997) *Cell Motil. Cytoskeleton 38*, 270−7.
23. Galletto, R., Rajendran, S., and Bujalowski, W. (2000) *Biochemistry 39*, 12959−69.
24. Gerlach, A. C., Gangopadhyay, N. N., and Devor, D. C. (2000) *J. Biol. Chem. 275*, 585−98.
25. Kwak, J., Wang, M. H., Hwang, S. W., Kim, T. Y., Lee, S. Y., and Oh, U. (2000) *J. Neurosci. 20*, 8298−304.
26. Ohkubo, S., Kumazawa, K., Sagawa, K., Kimura, J., and Matsuoka, I. (2001) *J. Neurochem. 76*, 872−80.
27. Hayashi, I., Oyama, T., and Morikawa, K. (2001) *Embo J. 20*, 1819−28.
28. Bilwes, A. M., Quezada, C. M., Croal, L. R., Crane, B. R., and Simon, M. I. (2001) *Nat. Struct. Biol. 8*, 353−360.
29. Cserpán, I., and Vas, M. (1983) *Eur. J. Biochem. 131*, 157−162.
30. Tompa, P., Hong, P. T., and Vas, M. (1986) *Eur. J. Biochem. 154*, 643−649.
31. Elõdi, P. (1958) *Acta Phys. Acad. Sci. Hung. 13*, 199−206.
32. Burton, K. (1959) *Biochem. J. 71*, 388−395.
33. Gupta, R. K., Gupta, P., Yashok, W. P., and Rose, Z. B. (1983) *Biochem. Biophys. Res. Comm. 117*, 210−216.
34. Larsson-Raznikiewicz, M. (1964) *Biochim. Biophys. Acta 85*, 60−68.
35. Krietsch, W. K., and Bücher, T. (1970) *Eur. J. Biochem. 17*, 568−575.
36. Fox, I. B., and Dandliker, W. B. (1956) *J. Biol. Chem. 221*, 1005−1017.
37. Szilágyi, A. N., and Vas, M. (1998) *Biochemistry 37*, 8551−8563.
38. Leslie, A. G. W. (1992) *Newslett. Protein Crystallogr. 26.*
39. Otwinowski, Z. (1993) in *Data Collection and Processing* (Sawyer, L., Isaacs, N., and Bailey, S., Eds.) pp 56−62, Daresbury Laboratories, Warrington, UK.
40. Navaza, J. (1994) *Acta Crystallogr., Sect. A 50*, 157−163.
41. CCP4. (1994) *Acta Crystallogr., Sect. D 40*, 760−763.
42. Brunger, A. T. (1992) *X-PLOR: Version 3.1; A System for Protein Crystallography and NMR*, Yale University Press, New Haven, CT.
43. Jones, T. A., Zou, J.-Y., Cowan, S. W., and Kjeldgaard, M. (1991) *Acta Crystallogr., Sect. A 47*, 110−119.
44. Riddles, P. W., Blakeley, R. L., and Zerner, B. (1979) *Anal. Biochem. 94*, 75−81.
45. Riddles, P. W., Blakeley, R. L., and Zerner, B. (1983) *Methods Enzymol. 91*, 49−60.
46. Dékány, K., and Vas, M. (1984) *Eur. J. Chem. 139*, 125−130.
47. Finkle, B. J., and Smith, E. L. (1958) *J. Biol. Chem. 230*, 669−690.
48. Bernstein, B. E., and Hol, W. G. (1998) *Biochemistry 37*, 4429−4436.
49. Harding, M. M. (1999) *Acta Crystallogr, Sect. D 55*, 1432−43.
50. Blake, C. C. F., and Rice, D. W. (1981) *Philos. Trans. R. Soc. London, Ser. A 293*, 93−104.
51. Larsson-Raznikiewicz, M. (1970) *Eur. J. Biochem. 17*, 183−92.
52. Vas, M., Merli, A., and Rossi, G. L. (1994) *Biochem. J. 301*, 885−891.
53. Molnár, M., and Vas, M. (1993) *Biochem. J. 293*, 595−599.
54. Mozzarelli, A., and Rossi, G. L. (1996) *Annu. Rev. Biophys. Biomol. Struct. 25*, 343−65.
55. Carugo, O., and Argos, P. (1997) *Protein Sci. 6*, 2261−2263.
56. Cao, Y., Musah, R. A., Wilcox, S. K., Goodin, D. B., and McRee, D. E. (1998) *Protein Sci. 7*, 72−8.
57. Geerlof, A., Schmidt, P. P., Travers, F., and Barman, T. (1997) *Biochemistry 36*, 5538−5545.
58. Hol, W. G., van Duijnen, P. T., and Berendsen, H. J. (1978) *Nature 273*, 443−6.
59. Laskowski, R. A., MacArthur, M. W., Moss, D. S., and Thorton, J. M. (1993) *J. Appl. Crystallogr. 26*, 283−291.

BI020210J